

BL43LXU

RIKEN Quantum NanoDynamics

1. Introduction

The bulk of the beamtime at BL43LXU [1] in 2021/2022 was for user experiments, but some testing and installation and commissioning of new equipment was also done (see below). The present report will, as usual, emphasize both the changes and the problems at the beamline, in an effort to provide a record of progress and to provide useful information to others working to develop SR instrumentation. One notes that the COVID-19 outbreak did impact operations. However, some remote work was carried out, and also some useful beamline tests and R&D. However, the limitations on international travel had a significant impact and prevented interested user groups from carrying out experiments.

2. Recent activities

Work at the experimental stations has largely been done by members of the Materials Dynamics Laboratory, with assistance on some projects by members of JASRI, and RIKEN. K. Taguchi also provided part-time help. BL43 also had some help from full-time members of the engineering team on specific tasks including standard start-up of the LN₂ cooling for the mirror and mono, and, sometimes, setup of sample refrigerators.

2-1. Optics Hutch & Related

The upstream components (electron orbit, IDs, mirrors, HHL mono) were stable during 2021/2022. The orbit-correction protocol operated smoothly, and there were no issues with the IDs. The high-heat-load mirror (M1) operated without changes -

and was stable when used. The BPM (SiC quadrant), just before the sample, is now well-integrated in standard BL operation.

2-2. Power Load Tests

The impact of power load on the monochromator performance was investigated by removing the first mirror, M1, that is installed upstream of the monochromator. This allowed us to reach high power on the mono and investigate the cooling performance. Results are shown in figure 1 where the usual (see [2]) minimum in the (333) rocking curve width at $3 \times 21.7 = 65$ keV is observed at a power load of about 450W. Notably, the peak in the meV-bandwidth intensity occurs at slightly smaller power loads, suggesting that the crystals are distorted even at the minimum.

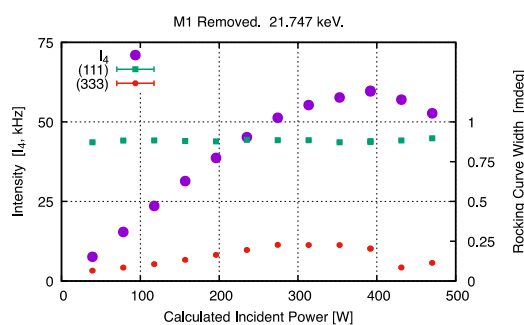


Fig. 1. Effect of power load on HHL mono performance when M1 is removed. The relative intensity of the meV beam (after multiple optical components) is shown on the left axis, while the measured FWHM of the rocking curves is indicated on the right axis.

2-3. Cryomagnet

We attempted to use the cryomagnet in two experiments. However, different issues (needle

valve failure, Attocube stage failure) only allowed partial operation. The previously motorized needle valve has now been replaced with a manual control, and the Attocube stage was replaced. However, despite a lot of work by BL staff, and help from the engineering team, it is now clear that additional staff is needed to operate the magnet effectively while maintaining operations for the remainder of the beamline.

2-4. Medium-Resolution Spectrometer

Most work during the year used the high-resolution spectrometer.

2-5. High-Resolution Spectrometer

This operated reasonably over most of the year.

2-6. Toward Higher Resolution

We are now working to achieve higher resolution. Our previous work demonstrated that 0.75 meV resolution at 25.7 keV was possible with spherical analyzers [3]. However, at that resolution, geometric contributions (e.g., due to the limited 10m spectrometer arm length) are a major contribution to the resolution. Therefore we are now investigating how to do better using a different setup. As a first step, we investigated the resolution possible with flat silicon crystals at high energy – in effect testing the silicon crystal quality. We did this using the Si(15 15 15) reflection at 29.656 keV which nominally should give a (two-crystal, convolved) resolution of ~ 0.23 meV near room temperature, or ~ 8 ppb, with an average extinction length of 2.4 mm. Figure 2 shows measurements over a portion of a test silicon crystal (average resistivity 5 kOhm-cm). The best resolution

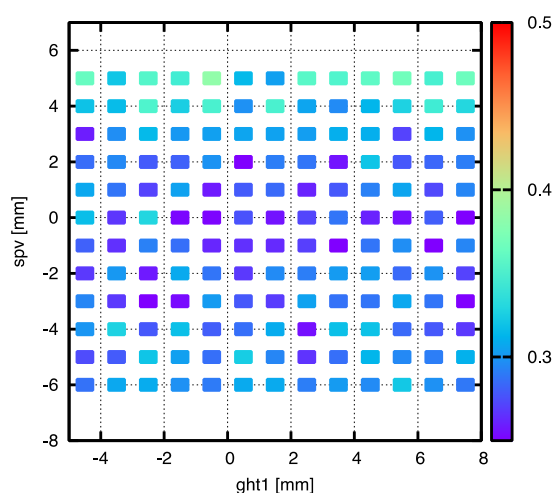


Fig. 2. Measured resolution (FWHM) in meV as a function of position over part of one carefully mounted silicon crystal. See text for discussion.

measured was ~ 0.26 meV, or about 1 ppb worse than that expected for ideal crystals. This resolution was, further, reasonably constant over $\sim \text{cm}^2$ areas giving us confidence that the silicon, if mounted with great care, will not limit resolution in our planned setup. We also note that mounting a temperature sensor ~ 30 mm from the x-ray spot was enough to significantly perturb the resolution at a level of a few ppb.

In a related measurement, figure 3 shows the average relative d-spacing variation in a silicon

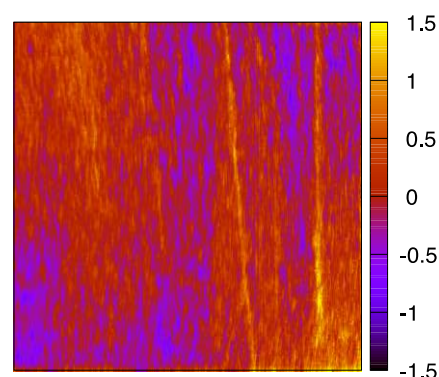


Fig. 3. d-spacing variation of a silicon crystal over a $7 \times 7 \text{ mm}^2$ area. 1 unit corresponds to a relative d-spacing change of 2.6×10^{-9} .

crystal over a region that is $7 \times 7 \text{ mm}^2$, now with continuous $\sim 0.1 \text{ mm}$ position resolution. One unit on the vertical scale corresponds to a 1 mK shift in reflecting temperature or a d-spacing change of 2.6 ppb . While definite structure can be seen it is actually remarkably uniform at the level of 1×10^{-9} .

2-7. 3-Layer Soller Screen

We continued to use Soller screens to help reduce backgrounds for high-pressure measurements. These are an alternative to a conventional Soller slit but are easier to fabricate when the required channel width/spacing is $\sim 0.1 \text{ mm}$ (see [4]). However, with the previous design, we found that there was some extraneous intensity making it through the assembly when the two-theta arm

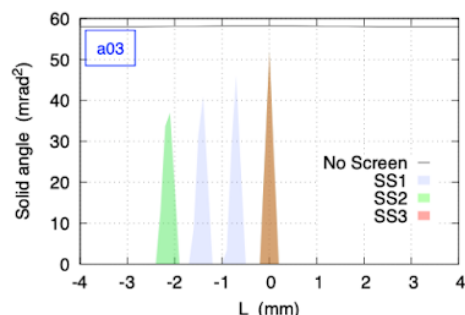


Fig. 4. Calculated performance of a 3-screen Soller screen. The horizontal axis, “L”, is the position of a scatterer along the incident beam while the vertical shows the solid-angle accepted into the analyzer. Adding the third screen (SS3) removes the extraneous intensity from a possible scatterer located at $L \sim -2 \text{ mm}$. This can be important when measuring samples in diamond anvil cells (DACs).

was moved to higher angles. Thus we now are considering replacing the 2-screen system with a 3-screen system. As the calculation shown in figure 4 indicates, this should help reduce backgrounds from scattering out of the center of the circles. However, it will require very careful

off-line alignment as we must manually place all 3 screens in-line to $\sim 0.01 \text{ mm}$ or better.

2-8. Area Detector Background Tests

We would like to use a pixel area detector for IXS, and, in particular, for the higher resolution setup discussed above. Extensive work [5], including both “time-slicing” processing and shielding, has shown it is possible to reduce backgrounds in a CdTe sensor-based detector to $\sim 0.005 \text{ s/cm}^2$ (while the value without such processing & shielding is $\sim 0.4 \text{ s/cm}^2$) for IXS. This makes us optimistic that higher-resolution experiments can be done. The importance of this can be seen

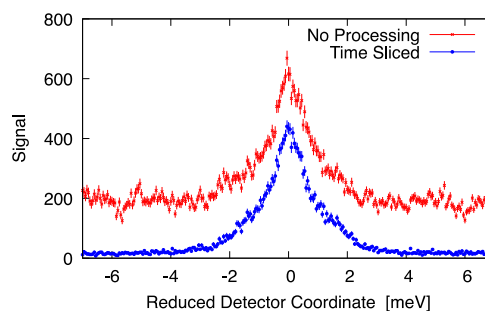


Fig. 5. IXS spectrum from ambient water measured using an area detector (Eiger2-1M CdTe) both with and without processing to remove background events. See text and [5]

in figure 5, where we present a measurement using an area detector both with and without additional processing. The signal in this case is the peak at near $x=0$. The improvement with processing, both in the reduction of background and in the improvement in statistical quality when cosmic ray tracks are removed, is clear.

Alfred Q.R. Baron and Ishikawa Daisuke
Materials Dynamics Group, Photon Science
Research Division, RIKEN SPring-8 Center

References:

- [1] A. Q. R. Baron, *SPring-8 Inf. News.* **15**, 14 (2010) <http://user.spring8.or.jp/sp8info/?p=3138> and A. Q. R. Baron, in *Synchrotron Light Sources Free. Lasers Accel. Physics, Instrum. Sci.*, edited by E. Jaeschke, et al. (Springer, Cham, 2016), p. 1643–1757.
See also <http://arxiv.org/abs/1504.01098>
- [2] A.I. Chumakov et al., *J. Synch. Rad.* **21** (2014) 315
<https://doi.org/10.1107/S1600577513033158>
- [3] Ishikawa, D., D. S. Ellis, Uchiyama H., and A. Q. R. Baron, *J. Synch. Rad.* **22**, 3 (2015).
<https://doi.org/10.1107/S1600577514021006>
- [4] A. Q. R. Baron, Ishikawa, D., Fukui, H. and Nakajima, Y. *AIP Proc.* **2054**, 20002(2019)
<https://aip.scitation.org/doi/abs/10.1063/1.5084562>.
See also <https://arxiv.org/abs/1807.03620>
- [5] A. Q. R. Baron and Ishikawa, D. to be published
(see also <https://arxiv.org/abs/2210.10219>)